University of Wollongong

Research Online

1-1-2005

Convergence rates comparison of sum-product decoding of RA codes under different message-passing schedules

Sheng Tong
Xidian University, sheng@uow.edu.au

Baoming Bai
Xidian University

Xinmei Wang
Xidian University

Convergence rates comparison of sum-product decoding of RA codes under different message-passing schedules

Abstract
In iterative decoding of turbo-like codes, serial schedule generally provides a much faster convergence rate compared with parallel schedule. With the aid of extrinsic information transfer (EXIT) charts, sum-product decoding of repeat accumulate (RA) codes under both message passing schedules is investigated as an example for verifying the above statement.

Keywords
product, sum, comparison, schedules, rates, passing, convergence, message, different, under, codes, ra, decoding

Disciplines
Engineering | Science and Technology Studies

Publication Details

Convergence Rates Comparison of Sum-Product Decoding of RA Codes Under Different Message-Passing Schedules

Sheng Tong, Baoming Bai, *Member, IEEE*, and Xinmei Wang, *Member, IEEE*

Abstract— **In iterative decoding of turbo-like codes, serial schedule generally provides a much faster convergence rate compared with parallel schedule. With the aid of extrinsic information transfer (EXIT) charts, sum-product decoding of repeat accumulate (RA) codes under both message passing schedules is investigated as an example for verifying the above statement.**

Index Terms— **Repeat accumulate (RA) codes, sum-product algorithm (SPA), extrinsic information transfer (EXIT) chart, message-passing schedule.**

I. INTRODUCTION

MESSAGE-PASSING schedules play an important role in the iterative decoding of turbo-like codes, especially in the convergence rate of iterative decoding. Different message-passing schedules lead to different convergence rates. Two commonly used schedules include serial (or two-way) one and parallel (or flooding) one. In general, serial schedule offers a much faster convergence rate compared to parallel schedule [2-6].

In [5], we have compared the convergence rates of Gallager codes under the two schedules. In this letter we analyze the convergence rates of sum-product decoding of RA codes under both serial and parallel schedules by using the EXIT chart technique.

II. EXIT CHART OF RA CODES

A. RA Codes

RA codes is a class of serially concatenated turbo-like codes, employing a rate-$1/q$ repeat codes as the outer code and a $1/(1 + D)$ accumulate code as the inner code linked by an interleaver [1]. The factor graph of a rate-1/3 RA code is shown in Fig. 1, which consists of 4 layers from top to bottom: namely, repeat codes (REPCs) layer, an interleaver, single parity check codes (SPCCs) layer, and another REPCs layer. However, the last two layers can also be viewed as an accumulate code (ACC) layer. These two different interpretations lead to the application of parallel schedule and serial schedule respectively.

B. EXIT Curves of Repeat Codes and Single Parity Check Codes

Assume an AWGN channel with BPSK modulation and noise variance σ_n^2. Let the binary random variables X with realization $x \in \{\pm 1\}$ denote the transmitted modulated symbol. The channel observation at the receiver is then $y = x + n$, where $n \sim N(0, \sigma_n^2)$. Define the log-likelihood ratio (LLR) Z obtained from the channel observation y as

$$Z := \ln\left(\frac{p(y|x = +1)}{p(y|x = -1)}\right) = \frac{2}{\sigma_n^2}y = \frac{2}{\sigma_n^2}(x + n) \quad (1)$$

Thus, the mutual information $I_Z = I(X; Z)$ between X and Z is given by [8]

$$I_Z(X; Z) = \frac{1}{2}\sum_{x=\pm 1}\int_{-\infty}^{+\infty} p_Z(\xi|X = x)$$

$$\times \log_2 \frac{2 \cdot p_Z(\xi|X = x)}{p_Z(\xi|X = -1) + p_Z(\xi|X = +1)}d\xi \quad (2)$$

Using the knowledge that $p_Z(\xi|X = x)$ is a Gaussian probability density function, (2) becomes [6,7,8]

$$J(\sigma = 2/\sigma_n) := I_Z(X; Z)$$
$$= 1 - \int_{-\infty}^{+\infty} \frac{e^{-(x - \sigma^2/2)^2/2\sigma^2}}{\sqrt{2\pi\sigma^2}} \log_2(1 + e^{-x})dx \quad (3)$$

For a code rate R, by (1) the variance of the LLR value Z is $\sigma_{ch}^2 = 4/\sigma_n^2 = 8R \cdot E_b/N_0$ [6,7]. Thus the mutual information can be written as $I_Z(X; Z) = J(\sigma_{ch})$.

Now, consider an $(n, 1, n)$ repeat code, for which the decoder operates by adding the input LLRs and outputting extrinsic information. The EXIT function of the repeat code is then calculated as follows [6,7].

a) If $n - 1$ input LLRs are from the inner edges and one from the channel, then

$$I_{E,REP}\left(I_A, \frac{E_b}{N_0}, n\right) = J\left(\sqrt{(n - 2)[J^{-1}(I_A)]^2 + \sigma_{ch}^2}\right) \quad (4a)$$

b) If all the LLRs are from inner edges, then

$$I_{E,REP}(I_A, n) = J\left(\sqrt{(n - 1)[J^{-1}(I_A)]^2}\right) \quad (4b)$$

Following the duality property for the binary erasure channel, the EXIT function for an $(n, n - 1, 2)$ single parity check code can be calculated as [6,7]

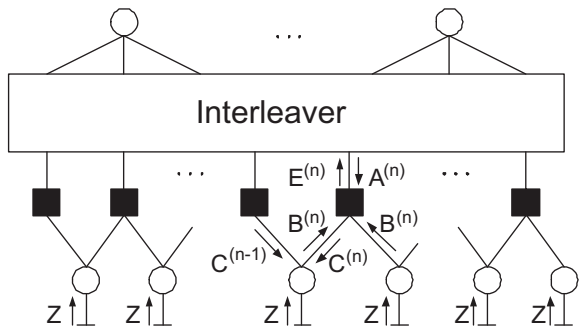$$I_{E,SPC}(I_A, n) = 1 - I_{E,REP}(1 - I_A, n) \quad (5)$$

Fig. 1. The factor graph for a rate-1/3 RA code (open circles denote variable nodes and filled squares denote parity check nodes).

Fig. 2. Sum-product decoding of the accumulate code under serial schedule.

Simulations show that this expression is an accurate approximation for the case of an AWGN channel [6,7]. For computer implementation, efficient approximations for the function $J(\cdot)$ and its inverse function $J^{-1}(\cdot)$ have been developed in [6], and thus the EXIT curves for both REPCs and SPCCs are easily accessible. In the following we use the two approximations in [6] to obtain the EXIT curves for REPCs and SPCCs.

C. EXIT Curves of RA Codes Under Parallel Schedule

With the reference to Fig.1, the iteration step of sum-product decoding of RA codes under parallel schedule is formulated as follows.

1) Upward pass:

$$B^{(n)} = Z + C^{(n-1)}, E^{(n)} = B^{(n)} \boxplus B^{(n)} \qquad (6a)$$

2) Downward pass:

$$A^{(n)} = E^{(n)} + E^{(n)}, C^{(n)} = A^{(n)} \boxplus B^{(n)} \qquad (6b)$$

where $C^{(0)}$ is initialized with 0, $\boxplus$ denotes the box-plus operation ($C = A \boxplus B \Leftrightarrow C = \ln\left[(e^{(A+B)} + 1)/(e^A + e^B)\right]$) and the superscript (n) denotes the nth iteration.

To draw the EXIT curves for RA codes under parallel schedule in a two-dimensional graph, we consider the two bottom layers of Fig.1, i.e., the SPCCs layer and the bottom REPCs layer, as a single layer, named SPC&REP layer. Thus, from (6) the EXIT function of SPC&REP layer is given by

$$\begin{aligned} I_{E,SPC\&REP}(I_A, E_b/N_0) &= I_{E,SPC}(I_B, 3) \\ &= I_{E,SPC}(I_{E,REP}(I_C, E_b/N_0, 3), 3) \\ &= I_{E,SPC}(I_{E,REP}(I_{E,SPC}(I_A, I_B, 3), E_b/N_0, 3), 3) \end{aligned} \qquad (7a)$$

where I_A, I_B and I_C denote the mutual information associated with A, B, C respectively. Note that according to (6) I_A and I_B are closely related by

$$I_A = I_{E,REP}(I_E, 3) = I_{E,REP}(I_{E,SPC}(I_B, 3), 3) \qquad (7b)$$

Using (7), the EXIT curve for SPC&REP layer, named ACC EXIT curve under parallel schedule, is plotted in Fig.3. Also shown is the EXIT curve of the top REPCs layer, denoted as REP EXIT curve, which is in fact the EXIT curve for a (3,1,3) repeat code in the absence of channel information.
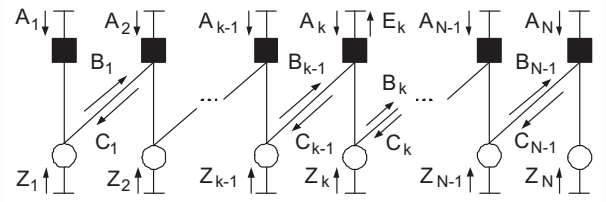
D. EXIT Curves of RA Codes Under Serial Schedule

Viewing the two bottom layers as an ACC, we can apply serial schedule, or two-way schedule, to decode the ACC using SPA as follows (see Fig.2).

1) Forward Pass:

$$B_k = B_{k-1} \boxplus A_k + Z_k, B_1 = A_1 + Z_1 \qquad (8a)$$

2) Backward Pass:

$$C_{k-1} = (C_k + Z_k) \boxplus A_k, C_{N-1} = Z_N \boxplus A_N \qquad (8b)$$

3) Output Extrinsic information:

$$E_k = B_{k-1} \boxplus (C_k + Z_k) \qquad (8c)$$

It can be rigorously proved that the above algorithm is equivalent to the BCJR algorithm [9] (see appendix or [3]). The EXIT curve for ACC under serial schedule is also plotted in Fig.3, which is obtained from simulation (for details refer to [8,5]). The decoding trajectories under both schedules are also shown in Fig.3, from which we can easily see that serial schedule provides a much faster convergence rate compared to parallel schedule. However, it should be noted that with the decrease of E_b/N_0 the ACC EXIT curve under serial schedule and that under parallel schedule finally merge, leading to the same threshold ($E_b/N_0 \approx 0.57$dB).

III. SIMULATION RESULTS AND CONCLUSIONS

A length-3×1024, rate-1/3 RA code is used for simulation, whose BER performance is plotted against E_b/N_0 in Fig.4. From Fig.4, it can be easily seen that sum-product decoding of the RA code under serial schedule really converges faster than under parallel schedule, which confirms the statement that serial schedule generally offers a faster convergence rate compared to parallel schedule.

APPENDIX
THE EQUIVALENCE OF SPA UNDER SERIAL SCHEDULE AND THE BCJR ALGORITHM

Proof: (see Fig.2.) In the proof below, we follow the conventional notations in the BCJR algorithm [9]. A similar proof can be found in [3].

(1) $\alpha_k(s)$ and B_k:

$$\ln \frac{\alpha_k(0)}{\alpha_k(1)} = \ln \frac{\alpha_{k-1}(0)\gamma_k(0,0) + \alpha_{k-1}(1)\gamma_k(1,0)}{\alpha_{k-1}(0)\gamma_k(0,1) + \alpha_{k-1}(1)\gamma_k(1,1)}$$

$$= \ln \left(\frac{\alpha_{k-1}(0)p(y_k^s|c_k^s=0)p(y_k^p|c_k^p=0)}{\alpha_{k-1}(0)p(y_k^s|c_k^s=1)p(y_k^p|c_k^p=1)} \right.$$

$$\left. \frac{+\alpha_{k-1}(1)p(y_k^s|c_k^s=1)p(y_k^p|c_k^p=0)}{+\alpha_{k-1}(1)p(y_k^s|c_k^s=0)p(y_k^p|c_k^p=1)} \right)$$

$$= \ln \frac{e^{\ln((\alpha_{k-1}(0))/(\alpha_{k-1}(1)))}e^{A_k}e^{Z_k} + e^{Z_k}}{e^{\ln((\alpha_{k-1}(0))/(\alpha_{k-1}(1)))} + e^{A_k}}$$

$$= \ln \frac{\alpha_{k-1}(0)}{\alpha_{k-1}(1)} \boxplus A_k + Z_k$$

Besides, $B_k = B_{k-1} \boxplus A_k + Z_k$ and $\ln \frac{\alpha_1(0)}{\alpha_1(1)} = \ln \frac{\alpha_0(0)}{\alpha_0(1)} \boxplus A_1 + Z_1 = \infty \boxplus A_1 + Z_1 = A_1 + Z_1 = B_1, \therefore B_k = \ln \frac{\alpha_k(0)}{\alpha_k(1)}$;

(2) $\beta_k(s)$ and C_k:

$$\ln \frac{\beta_k(0)}{\beta_k(1)} = \ln \frac{\beta_{k+1}(0)\gamma_k(0,0) + \beta_{k+1}(1)\gamma_k(0,1)}{\beta_{k+1}(0)\gamma_k(1,0) + \beta_{k+1}(1)\gamma_k(1,1)}$$

$$= \ln \left(\frac{\beta_{k+1}(0)p(y_{k+1}^s|c_{k+1}^s=0)p(y_{k+1}^p|c_{k+1}^p=0)}{\beta_{k+1}(0)p(y_{k+1}^s|c_{k+1}^s=1)p(y_{k+1}^p|c_{k+1}^p=0)} \right.$$

$$\left. \frac{+\beta_{k+1}(0)p(y_{k+1}^s|c_{k+1}^s=1)p(y_{k+1}^p|c_{k+1}^p=1)}{+\beta_{k+1}(1)p(y_{k+1}^s|c_{k+1}^s=0)p(y_{k+1}^p|c_{k+1}^p=1)} \right)$$

$$= \ln \frac{e^{\ln(\beta_{k+1}(0)/\beta_{k+1}(1))}e^{A_{k+1}}e^{Z_{k+1}} + 1}{e^{\ln(\beta_{k+1}(0)/\beta_{k+1}(1))}e^{Z_{k+1}} + e^{A_{k+1}}}$$

$$= \left(\ln \frac{\beta_{k+1}(0)}{\beta_{k+1}(1)} + Z_{k+1} \right) \boxplus A_k$$

Besides, $C_k = (C_{k+1} + Z_{k+1}) \boxplus A_{k+1}$ and $\ln \frac{\beta_{N-1}(0)}{\beta_{N-1}(1)} = (\ln \frac{\beta_N(0)}{\beta_N(1)} + Z_N) \boxplus A_N = (0 + Z_N) \boxplus A_N = Z_N \boxplus A_N = C_{N-1}. \therefore C_k = \ln \frac{\beta_k(0)}{\beta_k(1)}$;

(3) Extrinsic information E_k:

$$\ln \frac{P(u_k=0|\overline{y}_1^N)}{P(u_k=1|\overline{y}_1^N)}$$

$$= \ln \frac{\alpha_{k-1}(0)\gamma_k(0,0)\beta_k(0) + \alpha_{k-1}(1)\gamma_k(1,1)\beta_k(1)}{\alpha_{k-1}(0)\gamma_k(0,1)\beta_k(1) + \alpha_{k-1}(1)\gamma_k(1,0)\beta_k(0)}$$

$$= \ln \frac{e^{B_{k-1}}e^{A_k}e^{Z_k}e^{C_k} + e^{A_k}}{e^{B_{k-1}} + e^{Z_k}e^{C_k}}$$

$$= A_k + B_{k-1} \boxplus (C_k + Z_k).$$

$$\therefore E_k = B_{k-1} \boxplus (C_k + Z_k).$$

ACKNOWLEDGMENT

REFERENCES

[1] D. Divsalar, H. Jin, and R. J. McEliece, "Coding theorem for 'turbo-like' codes," in *Proc. 36th Annu. Allerton Conf. Commun. Control, Computing*, Sept. 1998, pp. 201-210.

[2] H. Kfir and I. Kanter, "Parallel versus sequential updating for belief propagation decoding," *Physica A*, 330(2003), pp. 259-270.
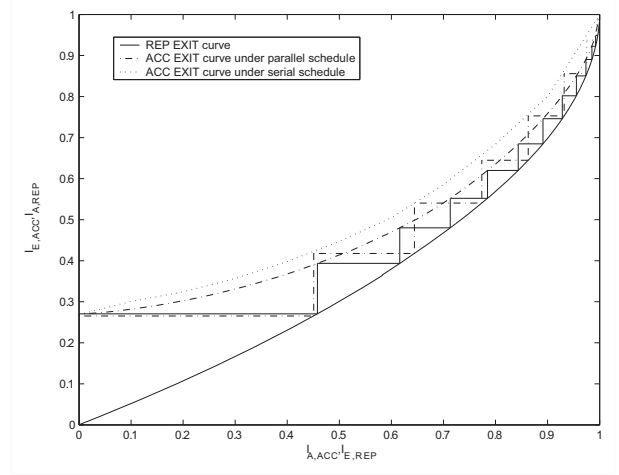

Fig. 3. EXIT curves for a rate-1/3 RA code decoded using SPA under serial and parallel schedules (E_b/N_0 = 2dB).
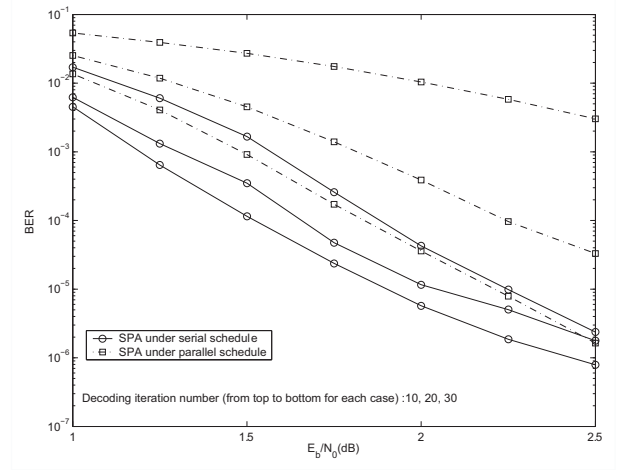

Fig. 4. BER performance of a length-3×1024, rate-1/3 RA code

[3] J. Li, K. R. Narayanan, and C. N. Georghiades, "An efficient decoding algorithm for cycle-free convolutional codes and its applications," in *Proc. IEEE Global Commun. Conf.*, Nov. 2001, pp. 1063-1067.

[4] J. Zhang and M. P. C. Fossorier, "Shuffled iterative decoding," accepted for publication in *IEEE Trans. Commun.*.

[5] S. Tong and X. Wang, "A simple convergence comparison of Gallager codes under two message-passing schedules," *IEEE Commun. Lett.*, vol. 9, pp. 249-251, Mar. 2005.

[6] S. ten Brink, G. Kramer, and A. Ashikhmin, "Design of low-density parity-check codes for multi-antenna modulation and detection," *IEEE Trans. Commun.*, vol. 52, pp. 670-678, Apr. 2004.

[7] S. ten Brink and G. Kramer, "Design of repeat-accumulate codes for iterative detection and decoding," *IEEE Trans. Signal Processing*, vol. 51, pp. 2764-2772, Nov. 2003.

[8] S. ten Brink, "Convergence behavior of iteratively decoded parallel concatenated codes," *IEEE Trans. Commun.*, vol. 49, pp. 1727-1737, Oct. 2001.

[9] L. R. Bahl, J. Cocke, F. Jelinek, and J. Raviv, "Optimal decoding of linear codes for minimizing symbol error rate," *IEEE Trans. Inform. Theory*, vol. 49, pp. 284-287, Mar. 1974.